Biodiesel Effects on Particulate Radiocarbon (^{14}C) Emissions From a Diesel Engine

Maren Bennett[1], John Volckens[2*], Rudy Stanglmaier[1], Ann P. McNichol[3], William D. Ellenson[4] and Charles W. Lewis[5] (deceased)

[1]Department of Mechanical Engineering, Engines and Energy Conversion Laboratory, Colorado State University, Fort Collins, Colorado

[2]Department of Environmental and Radiological Health Sciences, Colorado State University, Fort Collins, Colorado

[3]Woods Hole Oceanographic Institution, Woods Hole, Massachusetts

[4]Alion Science and Technology, Research Triangle Park, North Carolina

[5] National Exposure Research Laboratory, U.S. Environmental Protection Agency, Research Triangle Park, North Carolina

Address correspondence to: Dr. John Volckens, Department of Environmental and Radiological Health Sciences, Colorado State University, Fort Collins, CO 80521; (p) 970-491-6341; (f) 970-491-2940; john.volckens@colostate.edu

ABSTRACT

The relative amount of ^{14}C in a sample of atmospheric particulate matter (PM), defined as percent modern carbon (pMC), allows EPA to infer the fraction of PM derived from anthropogenic pollution sources. With increased use of biofuels that contain ^{14}C, the main assumption of the two-source model, that ^{14}C is solely derived from biogenic sources, may become invalid. The goal of this study was to determine the ^{14}C content of PM emitted from an off-highway diesel engine running on commercial grade biodiesel.

Tests were conducted with an off-highway diesel engine running at 80% load fueled by various blends of soy-based biodiesel. A dilution tunnel was used to collect PM_{10} emissions on quartz filters that were analyzed for their ^{14}C content using accelerator mass spectrometry. A mobility particle sizer and 5-gas analyzer provided supporting information on the particle size distribution and gas-phase emissions.

The pMC of PM_{10} aerosol increased linearly with the percentage of biodiesel present in the fuel. Therefore, PM emissions resulting from increased combustion of biodiesel fuels will likely affect contemporary ^{14}C apportionment efforts that attempt to split biogenic vs. anthropogenic emissions based on aerosol-^{14}C content. Increasing the biodiesel fuel content also reduced emissions of total hydrocarbons (THC), PM_{10} mass, and particulate elemental carbon. Biodiesel had variable results on oxides of nitrogen (NO_x) emissions.

INTRODUCTION

Biodiesel, a renewable alternative to petroleum-based diesel fuel, continues to see increased use globally. Europe is the global leader in biodiesel production with an estimated 1.85 billion gallons produced in 2006 (Beckman 2006). Biodiesel is expected to reach 6% of total on-road transportation fuel consumption in Europe by 2010 (Online 2007). Some experts believe that Europe, Brazil, China and India have the potential to replace up to 20% of all on-road diesel with biodiesel, while the US Department of Energy estimates that readily available feedstocks in the US are capable of displacing roughly 5% of on-road diesel (Online 2007, US DOE 2007). Commercial scale production of biodiesel in the United States began as early as 1990. Total production has grown from 500,000 gallons, or less than 0.05% of the diesel market share, in 1999 to at least 25 million gallons in 2004 and an estimated 80 million gallons in 2005. U.S. biodiesel production reached approximately 300 million gallons in 2006 and is estimated to reach 750 million gallons by the end of 2007, or approximately 1.2% of the diesel market share (Online 2007). Although biodiesel production is relatively small compared to overall diesel use, it is believed that the biodiesel market will continue to grow even more quickly as new feedstocks are developed.

Biodiesel is produced by transesterfying long chain fatty acids present within raw, biogenic oils to form methyl-ester derivatives more suitable for diesel combustion (Pahl 2004). Much of the early biodiesel production in the U.S. was from soybean oil. As demand for soy meal increased, farmers began searching for a means to unload their

surplus oil. The U.S. is the largest producer of soybeans in the world and some estimate that over 90% of current U.S. biodiesel production utilizes soybean oil (Gartner 2007).

Many studies have noted strong reductions in total hydrocarbons (THC), particulate matter (PM), and carbon monoxide (CO) emissions as a result of biodiesel fuel combustion (Schumacher et al. 2001; Krahl et al. 2005). Reductions in THC emissions by 10% and 45% have been shown for B35 and B100, respectively, when compared to traditional petrodiesel (Schumacher et al. 2001; Krahl et al. 2005). Carbon monoxide (CO) emissions have been shown to decrease by up to 48% when running on B100 compared to petrodiesel (Schumacher et al. 2001; Krahl et al. 2005). Biodiesel is believed to decrease CO and THC emissions because of the esterfied oxygen in the fuel, which increases the completeness of combustion.

Emissions of nitrogen oxides (NO_x) are believed to increase with the increased proportion of biodiesel in the fuel, although there is a great deal of contradicting information on the magnitude and direction of this effect (Sheehan et al. 1998; McCormick et al. 2001; Monyem et al. 2001; Schumacher et al. 2001; Krahl et al. 2005). While some have attributed the increase in biodiesel NO_x formation to higher combustion temperatures, Monyem et al. (Monyem et al. 2001) reported biodiesel flame temperatures lower than that of petrodiesel. Increased NO_x observed with biodiesel could also be caused by fuel properties such as oxygen content and cetane number. One theory states that more oxygen available in the reaction zone during combustion leads to a greater likelihood of NO_x formation (Monyem et al. 2001). Biodiesel has a roughly 10% higher oxygen content than typical diesel fuel (Pahl 2004); the exact difference depends on the feedstock and production process. Combustion timing has proven to be more advanced

for biodiesel than for diesel fuel due to its higher cetane number (Monyem et al. 2001). Cetane number is a measure of ignition quality; a higher value indicates a shorter ignition delay or earlier injection timing. Typically, early injection correlates with higher combustion temperatures, although the shorter ignition delay could also cause less premixed combustion. Monyem et al. identified this occurrence as a possible source of NO_x formation in naturally aspirated and lightly turbocharged engines (Monyem et al. 2001). However, McCormick et al. indicate decreased NO_x emissions with increasing cetane number (McCormick et al. 2001). Clearly, more research is warranted in this area.

One common method for determining sources of airborne particulate matter is based on a two-component model that classifies organic aerosol carbon as fossil (dead) carbon or modern (living) carbon (Currie et al. 1980). Living and recently living material is assumed to be in equilibrium with the atmosphere, which contains an approximate concentration of 1.2 radioactive carbon atoms (^{14}C) per 1012 ordinary carbon atoms (^{12}C + ^{13}C). This equilibrium is maintained by organisms that utilize carbon dioxide (CO_2) for photosynthesis. Cosmic irradiation of nitrogen in the upper atmosphere occurs with regular frequency, producing radioactive ^{14}C atoms. These carbon atoms combine with oxygen to form CO_2. Since the half-life of ^{14}C is about 5730 years, fossil fuels, which are typically over a million years old, are almost completely devoid of ^{14}C (Currie 2004). Petroleum contains less than 1 part per 10^{15} atoms of ^{14}C (Buchholz et al. 2003). The lack of radioactive carbon present in fossil fuels allows researchers to infer the fraction of carbon in ambient aerosol from anthropogenic, fossil-fuel combustion by comparing a sample's radioactive fraction to the current radioactive fraction present in the atmosphere (Lemire et al. 2002; Bench et al. 2004; Endo et al. 2004; Szidat et al. 2004; Szidat et al.

2004; Tanner et al. 2004; Lewis et al. 2006). While this technique is not capable of defining all anthropogenic sources (i.e., wood smoke for residential heating contains modern carbon), it is useful for defining the contribution from mobile-sources (i.e., cars, trucks, small-engines) to ambient PM. However, a main assumption of this two-source model, that mobile-source emissions from anthropogenic sources lack radioactive carbon, may soon become invalid. As nations seek alternative fuel sources, many biofuels are being utilized such as biodiesel, ethanol and syn-gas liquids. These recently living fuels contain measurable levels of ^{14}C that, when combusted, may bias the two-component model for source apportionment. Note also, In areas where

Cheng et al. studied PM emissions from a four-stroke diesel engine as a function of biodiesel percentage and noted that percent modern carbon (pMC) tends to increase with increasing biodiesel blend ratio (Cheng et al. 2003). However, Cheng et al. focused only elemental carbon (EC) and chose to ignore the contribution of organic carbon (OC) to pMC (or ^{14}C). Interestingly, increasing the proportion of biodiesel in the fuel tended to decrease EC emissions and increase total carbon (TC) emissions, inferring an increase in OC emissions from biodiesel usage. However, these authors did not account for organic sampling artifacts that tend to bias OC measurement on quartz fiber filters.

Lewis et al. reported that the proportion of ^{14}C associated with $PM_{2.5}$ emissions from small, two-stroke engines powered by a gasoline/ethanol mix are drastically lower than expected from the ^{14}C content of the fuel (Lewis et al. 2006). While this phenomenon contradicts that of Cheng et al., there are important differences to note among the two studies. The Lewis et al. two-stroke study may not translate well to other forms of internal combustion such as four-stroke compression ignition (i.e., diesel

combustion). For example, the majority of particulate matter generated from handheld, two-stroke engines can be attributed to emissions of unburned oil, which lacks modern carbon. In small, two-stroke engines, oil is blended directly into the gasoline fuel. A portion of this fuel mixture is directly emitted as a scavenging loss from small two-stroke engines, and this material quickly condenses to form PM. Also, biogenic ethanol is quite different from biodiesel; the former is a 2-carbon species, while the latter is a distribution of long-chain fatty acids centered around C_{16}.

The primary goal of this study was to determine the ^{14}C content of PM emissions (OC + EC) from a typical diesel engine operating on commercial-grade biodiesel and to test the hypothesis that biodiesel has the potential to bias ^{14}C apportionment techniques. This study expands upon the work of Cheng et al. by testing a wider range of biodiesel fuel blends at a higher dilution ratio and also by accounting for OC contributions (artifact corrected) to PM emissions from a diesel engine.

EXPERIMENTAL METHODS

Emissions Measurements

Engine Parameters.

A John Deere 4024T, off-highway diesel engine meeting U.S. Tier 2 emissions guidelines was used for all testing. This 4-cylinder engine has 2.4 L displacement, turbocharged aspiration, and is rated at 56 bhp (41.8 kW) for applications operating under a constant load and speed. The engine was connected to an eddy-current dynamometer, which was set to provide an engine load at 80% of maximum at a speed of 2400 rpm.

Fuel and Oil.

Four fuel blends were used: standard diesel (B0), 19% biodiesel (B19), 32% biodiesel (B32) and 83% biodiesel (B83). To avoid contamination of fuel blends, the engine ran on the new blend for at least 20 minutes prior to measurement to purge the transfer line and internal engine compartments of fuel from previous runs. This duration was recommended by engineers at John Deere to ensure that 100% of the tested fuel came from the fuel reservoir and not from within the engine. A random testing order was employed to avoid the influence of any systematic sources of error. Fuels samples were taken directly from the test reservoir throughout the testing period and stored in amber glass containers for later modern carbon analysis. John Deere PLUS-50 Supreme Motor Oil – SAE 15W-40 was used in the engine. Oil levels were maintained throughout experimentation and the same oil was used for all tests. These test parameters are summarized in Table 1.

Sampling.

The dilution tunnel used for sampling, shown in Figure 1, is a modified version of the original Hildemann design (Hildemann et al. 1989). Engine emissions were drawn from the exhaust manifold (post-turbocharger) through an isokinetic sampling probe and relayed to the dilution tunnel through a heated sample line (150ºC) to prevent water condensation prior to dilution. Background dilution air was cleaned by use of a high efficiency particulate air filter followed by an activated charcoal filter to remove any organic contaminates that could bias the collected sample. Diluted emissions were then directed around a U-shaped channel where turbulent mixing occurred. The diluted mixture, at a 50:1 dilution ratio, was directed into a 320 liter residence chamber and equilibrated for approximately 80 seconds prior to sampling. An excess air pump was

installed on one port to control the residence time. Sampling ports located at the base of the chamber provide access to various sampling devices. The average run duration was 4 hours long and no two fuels were tested on the same day.

A LabVIEW data acquisition system provided control and recording capabilities for the dilution system. Mass-flow controllers regulated airflow through the filter packs, maintaining a rate of 28.3 L/min for each. Temperatures were automatically recorded via thermocouple relays at three points along the flow path ending in the residence chamber where a humidity reading was also taken. Background air temperature, pressure and humidity were also recorded for each test.

Filter samples were drawn through Teflon-coated aluminum cyclones (URG Corp., Chapel Hill, N.C) to remove particles larger than 10 μm aerodynamic diameter (PM_{10}). Each cyclone was followed by a dual-stage stainless steel filter holder (URG-2000-30FDT). Filters were contained in 47 mm delrin filter cassettes that could easily be changed out between testing. Both filter packs and cassettes were cleaned prior to each test with a 1:1:1 volumetric mixture of acetone:hexane:dichloromethane and stored in fresh, sealed bags prior to use each day.

Samples for the radiocarbon and OC/EC analyses were collected on quartz filters that had been baked at 550°C for 12 hours prior to use. Collection of organic PM is complicated by the presence of semi-volatile compounds that exist in both gas and particulate phases at atmospheric conditions. Sampling artifacts associated with these compounds include evaporation of particle-associated organics from the filter surface (negative artifact) and adsorption of gas-phase organics onto the filter (positive artifact) (Turpin et al. 2000). Quartz filters have a large total surface area, therefore positive

artifacts due to adsorption are considered the dominant problem, especially for source profiling. For these tests, negative artifacts were considered less problematic since the aerosol was allowed to equilibrate prior to sampling and the sampled concentration remained relatively constant throughout each test.

The amount of adsorbed organic vapor was estimated by sampling through a second filter pack containing a Teflon-quartz filter combination. The front Teflon filter is assumed to collect 100% of the PM; the backup quartz filter is therefore exposed only to gas-phase organic compounds (Taft et al. 1985; McDow et al. 1990; Turpin et al. 2000). This backup quartz filter acts as a surrogate to estimate the magnitude of the positive artifact. Particulate OC was determined by subtracting the amount of OC detected on the backup quartz filter from the OC detected on the front quartz filter. Both Teflon and quartz filter blanks were carried for each test. Each blank was placed into the filter housing to account for cross-contamination between runs and was tested for organic carbon content.

Particle size distributions were measured during each test with a mobility particle sizer equipped with a long differential mobility analyzer (SMPS +C, Grimm Inc., Douglasville, GA). Prior to each run, a particle size scan for number concentration and particle contamination was conducted within the tunnel using the GRIMM instrument. Particle concentrations in the system before tests were approximately two orders of magnitude lower than when the engine was running.

A second probe was inserted into the exhaust stream, downstream of the isokinetic PM sampling probe, to draw a sample for the 5-gas analyzer. Condensation was prevented by heating (110°C) the transfer line between the exhaust manifold and the

emissions rack. Random, 5-minute data sets were averaged providing overall CO, CO_2, THC, NO_x & O_2 concentrations. Infrared radiation adsorption was used by the analyzer to determine relative CO and CO_2 concentrations. The concentration of THCs was measured using a flame ionization detection method. Chemiluminescence method of detection allowed NO_x concentrations to be measured while a paramagnetic technique was used to determine O_2 concentrations.

Filter Analysis

All filters were handled with fresh, neoprene gloves and pre-cleaned laboratory tweezers. Post testing, filters were kept in sealed, plastic Petri dishes and immediately stored at or below -40°C, with the exception of the Teflon filters, which were first weighed to the nearest microgram. All filters to be sent out for further testing were packed in ice and shipped overnight-delivery.

Samples were analyzed for ^{14}C content by the National Ocean Sciences Accelerator Mass Spectrometry Facility in Woods Hole, MA. A special punch was used to remove a rectangular 1.0 x 1.5 cm section of the filter. For very heavily loaded (black) filters, two sections were punched out from the same filter. Punched segments were placed into aluminum-lined covered Petri dishes with labeling as appropriate. The remaining fractions were also put into aluminum-lined Petri dishes with labeling as appropriate.

The radiocarbon analysis methodology differs depending on the amount of carbon present in the sample. To determine this information, filter segments were first analyzed for OC/EC content using the NIOSH method 5040 thermal-optic analysis (NIOSH 1995).

For heavily loaded filters (black), an additional analysis was performed in which a small quantity of sample material (“smear sample”) was applied to a clean quartz filter segment. This latter sample was used to provide a better breakdown between OC and EC for the original heavily loaded sample section.

In accelerator mass spectrometry, the carbon derived from a sample is compressed into a small cavity in an aluminum "target" that acts as a cathode in the ion source. The sample surface is sputtered with heated cesium and the ions produced are extracted and accelerated through the mass spectrometry system. After acceleration and removal of electrons, the emerging positive ions are magnetically separated by mass and the ^{12}C and ^{13}C ions are measured in Faraday Cups where their relative currents are recorded. Simultaneously, the ^{14}C ions are recorded in a gas ionization counter, so that instantaneous ratios of ^{14}C to ^{12}C and ^{13}C are determined. These raw signals are then used to determine the amount of modern carbon in the sample, which also indicates the radiocarbon age.

RESULTS AND DISCUSSION

The OC/EC results are compiled in Table 2 along with the data of Cheng et al. for comparison. Increasing the biodiesel blend ratio led to a decrease in TC, which is contrary to that observed by Cheng, who reported increased OC emissions with higher blends of biodiesel. However, the Cheng et al. data may be biased by the low dilution factor used (6.5:1) and a lack of adsorption artifact correction (Robinson et al., 2007). A reduced dilution factor often increases the measured OC content on filters, due to a shift

in gas-particle equilibrium dynamics. There is no statistically significant trend in OC emission rates reported here. For both studies, EC emissions decrease with an increasing proportion of biodiesel. A linear regression between EC and biodiesel percentage, shown in Figure 2, is significant at the 95% confidence interval (p-value = 0.04). Emissions of total carbon (TC = EC + OC) correlate well with gravimetric mass determined by Teflon filters, indicating a reasonable mass balance and lending credence to the semivolatile adsorption correction used.

To determine the pMC associated with PM_{10} emissions we must first correct for the positive adsorption artifact. Assuming that the front filter is exposed to modern particulate carbon and adsorbed gas-phase modern OC, while the back up filter is only exposed to gaseous modern OC, the corrected pMC in the particulate carbon is determined as follows:

$$pMC_{PC} = \frac{pMC_{front} \cdot M_{TC,front} - pMC_{back} \cdot M_{TC,back}}{M_{PM\_OC}} \qquad [1]$$

where, pMC_{PC} = percent of particulate carbon that is modern

pMC_{front} = percent of modern carbon measured on the front filter

$M_{TC,front}$ = mass of total carbon measured on the front filter

pMC_{back} = percent of modern carbon measured on the back filter

$M_{TC,back}$ = mass of total carbon measured on the back filter

M_{PM_OC} = mass of OC measured on the front filter corrected for adsorption

While this equation does not account for the presence of particulate carbon within the filtered dilution air, preliminary tests indicated that this error was negligible. The OC concentrations measured on the blanks was, on average, 2% of that collected by the filters. There was no EC contamination detected upon analysis of filter blanks.

Table 3 lists all pMC measurements for each fuel blend, as well as corrected values for particulate carbon. While the corrected pMC_{PC} is consistently much lower than the uncorrected pMC_{front}, the correction is not as significant as the study by Lewis et al. which showed a 50% reduction. The pMC_{PC} emissions are strongly correlated to the percentage of biodiesel fuel used and the pMC of the fuel. This relationship, shown in Figure 2, is significant at the 99.9% confidence interval (p-value < 0.0001). The EC-associated pMC from biodiesel, as reported by Cheng et al., is also shown in Figure 3 for comparison. Results from the two studies are remarkably similar, despite the difference in methodologies, indicating that modern carbon in the fuel is likely distributed equally among both OC and EC fractions.

Adsorbed carbon measured on the backup quartz filter in the current study appears to contain a larger proportion of modern carbon than the front quartz filter, as seen in Table 3. Some of this phenomenon can be explained by the fact that a portion of the lubricating oil from the engine, which lacks ^{14}C, is likely to partition into the particle phase upon cooling of the exhaust and become trapped by the front filter. The backup filter, however, is exposed only to gas-phase volatile and semivolatile compounds that are more likely derived from the fuel, which contains modern carbon.

Some modern carbon was detected on the filter samples for pure petrodiesel, as seen in Table 3, indicating a possible source of contamination. The likely explanation for

this occurrence is that biodiesel vapor escaped from the biodiesel fuel sump (located about 20 feet from the dilution tunnel) and was drawn into the system along with the dilution air. Such vapor likely absorbed to the quartz filters via the gas-phase adsorption artifact and could explain why the backup filters are so high in C_{14} or pMC. Our attempt to remove vapor intrusion into the tunnel through an activated charcoal bed may have been only partially effective. Residual modern carbon also may have been present within the engine from a previous test, however, this should have had little effect. With a fuel consumption rate of approximately 10 g/s, the 20 minute purge time should have cleared internal engine components of any fuel residuals. Further, the B0 tests were approximately three hours long, meaning that residual modern carbon within the engine could contribute, at most, less than a few percent of the total fuel volume consumed. Whatever the cause of this discrepancy, when the data are corrected for a vapor adsorption artifact (using equation 1 and shown on the left hand side of Table 3) the calculation of pMC becomes approximately 2% for the B0 tests, as expected.

No statistically significant trends were observed in O_2 or CO_2 emissions as a function of biodiesel percentage. NO_x emissions appeared to increase slightly with increasing biodiesel content, although the positive trend is only significant at the 50% confidence interval. THCs show a significant decreasing trend as the percentage of biodiesel increases while CO concentrations show a slight inverse relationship, as seen in Figure 4. A summary of average 5-gas emissions data can be found in Table 4.

Particle size distribution results are presented in Figures 5 and 6. Data for each blend are compared based on mobility diameter counts as measured by the SMPS. A substantial decrease in the total number concentration for B83 compared to B0 can be

seen in Figure 5. The reduced count data for B83 also correlates well with lower mass emissions (compared to B0), as seen in Figure 1. An important parameter to compare for each blend is the count median diameter (CMD), which represents the 50% particle size, by count. Particle size is important because it determines the overall behavior of the aerosol once released to the atmosphere. As the percentage of biodiesel increases, the CMD decreases by almost 20% for B83 compared to petrodiesel, as seen in Figure 6. The linear regression is significant at the 99% confidence interval (p-value of 0.01). This result is comparable to another study in which the geometric number mean diameter of the accumulation mode was found to decrease from 80 to 62 nm with the use of B100 (Jung et al. 2006). The decrease in diameter could be a result of the higher oxidation rate of biodiesel particles compared to diesel particles (Jung et al. 2006). Decreasing initial particle concentration as biodiesel percentage increases could also lead to the decrease in the final particle diameter. Fewer primary particles in the exhaust stream will lead to a decrease in the particle coagulation rate, preventing large agglomerates from forming as the aerosol approaches equilibrium. It is important to note that dilution conditions can affect both particle formation and agglomeration processes (Kittelson et al. 2005) and the dilutions ratios tested here were lower than ambient levels encountered on-road. However, we maintained the same level of dilution was for all tests and for each blend tested.

CONCLUSIONS

Levels of ^{14}C in PM_{10} emitted by the combustion of biodiesel blends in off-highway diesel engines increases with increased percentages of biodiesel in the fuel. Due to the high levels of ^{14}C in biodiesel emissions, the EPA's current two-source apportionment methods will be biased in areas with significant biodiesel usage. While it can be assumed that heavy-duty and light-duty passenger diesel engines would produce similar results, it may be valuable to test other engine sizes.

Biodiesel emissions were shown to be cleaner than regular diesel emissions due to a substantial decrease in THC emissions and total PM mass emission rates. No significant trends were observed for NO_x, CO, CO_2, or O_2. While less EC was emitted as the percentage of biodiesel increased, there was no clear trend in OC emission rates. Particle size was also shown to decrease by almost 20% with increased biodiesel. This phenomenon could be attributed to a lower initial number concentration in-cylinder or reduced size of primary particles.

ACKNOWLEDGMENTS

We thank the Engines and Energy Conversion Laboratory at the Colorado State University for providing the engine test bed and funding towards the dilution tunnel upgrades. In addition, Kris Quillen and Dan Mastbergen of the engines lab provided a great deal of technical support. Recognition should also be given to the National Ocean Sciences Accelerator Mass Spectrometry facility in Woods Hole, MA for the filter analysis through support from the National Science Foundation Cooperative Agreement number, OCE-9807266.

NOMENCLATURE

B100 – Pure Biodiesel (no petroleum)

bhp – Brake Horsepower

^{14}C – Radioactive Carbon Isotope

CMD – Count Median Diameter

CO – Carbon Monoxide

CO_2 – Carbon Dioxide

EC – Elemental Carbon (black)

kW – Kilowatt

NIOSH – National Institute for Occupational Safety and Health

NO_x – Oxides of Nitrogen

OC – Organic Carbon

$PM_{2.5}$ – Particulate Matter less than 2.5 μm in diameter

PM_{10} – Particulate Matter less than 10 μm in diameter

pMC – Percent Modern (living) Carbon

ppm – Parts per Million

SMPS – Scanning Mobility Particle Sizer

TC – Total Carbon

THC – Total Hydrocarbons

REFERENCES

1. Beckman, C. (2006). "Bi-Weekly Bulletin: Biodiesel." Agriculture and Agri-Food Canada 19(15).
2. Bench, G. and P. Herckes (2004). "Measurements of Contemporary and Fossil Carbon Contents of PM2.5 Aerosols: Results from Turtleback Dome, Yosemite National Park." Environmental Science and Technology 38(10): 2424-2427.
3. Buchholz, B. A., R. W. Dibble, et al. (2003). "Quantifying the contribution of lubrication oil carbon to particulate emissions from a diesel engine." SAE Technical Paper 2003-01-1987.
4. Cheng, A. S., B. A. Buchholz, et al. (2003). "Isotopic Tracing of Fuel Carbon in the Emissions of a Compression-Ignition Engine Fueled with Biodiesel Blends." SAE Technical Paper 2003-01-2283.
5. Currie, L. A. (2004). "The Remarkable Metrological History of Radiocarbon Dating [II]." Journal of Research of the National Institutes of Standards and Technology 109(2): 185-217.
6. Currie, L. A., G. A. Klouda, et al. (1980). "Mini-radiocarbon measurements, chemical selectivity, and the impact of man on environmental pollution and climate." Radiocarbon 22(2): 349-362.
7. Endo, M., N. Yamamoto, et al. (2004). "14C Measurement for Size-Fractionated Airborne Particulate Matter." Atmospheric Environment 38(36): 6263-6267.
8. Gartner, J. (2007). Biodiesel Boom Well-Timed. Wired. Accessed February 21, 2007: http://www.wired.com/news/autotech/0,2554,63635,00.html
9. Hildemann, L., G. R. Cass, et al. (1989). "A dilution stack sampler for collection of organic aerosol emissions – design, characterization and field tests." Aerosol Science and Technology 10: 193-204.
10. Jung, H., D. B. Kittelson, et al. (2006). "Characteristics of SME Biodiesel-Fueled Diesel Particle Emissions and the Kinetics of Oxidation." Environmental Science and Technology 40: 4949-4955.
11. Kittelson, D.B., W.F. Watts, et al. (2006). “On-road and laboratory evaluation of combustion aerosols—Part1: Summary of diesel engine results.” Journal of Aerosol Science. 37(8): 913-930.
12. Krahl, J., A. Munack, et al. (2005). "The Influence of Fuel Design on the Exhaust Gas Emissions and Health Effects." SAE Technical Paper 2005-01-3772.
13. Lemire, K. R., D. T. Allen, et al. (2002). "Fine Particulate Matter Source Attribution for Southeast Texas using 14C/13C Ratios." Journal of Geophysical Research 107(D22): 4613.
14. Lewis, C., J. Volckens, et al. (2006). "Absence of ¹⁴C in PM2.5 Emissions from Gasohol Combustion in Small Engines." Aerosol Science & Technology 40(9): 657.
15. McCormick, R. L., M. Graboski, et al. (2001). "Impact of Biodiesel Source Material and Chemical Structure on Emissions of Criteria Pollutants from a Heavy-Duty Engine." Environmental Science and Technology 35: 1742-1747.

16. McDow, S. R. and J. J. Huntzicker (1990). "Vapor adsorption artifact in the sampling of organic aerosol: Face velocity effects." Atmos. Environ. 24A(10): 2563-2571.
17. Monyem, A., J. H. Van Gerpen, et al. (2001). "The Effect of Timing and Oxidation on Emissions from Biodiesel-Fueled Engines." Transactions of ASAE 44: 35-42.
18. NIOSH (1995). Analytical Method No. 5040. Cincinnati, OH, National Institute for Occupational Safety and Health.
19. Online, E. M. (2007). Biodiesel 2020: A Global Market Survey. Accessed February 5, 2007: http://www.emerging-markets.com/biodiesel/default.asp
20. Pahl, G. (2004). Biodiesel: Growing a new Energy Economy. White River Jct., VT, Chelsea Green Publishing.
21. Robinson, A. L., N. M. Donahue, et al. (2007). "Rethinking Organic Aerosols: Semivolatile Emissions and Photochemical Aging." Science 315(5816): 1259-1262.
22. Schumacher, L., W. Marshall, et al. (2001). "Biodiesel emissions data from series 60 DDC engines." Transactions of the ASAE 44(6): 1465-1468.
23. Sheehan, J., V. Camobreco, et al. (1998). An overview of biodiesel and petroleum diesel life cycles. NREL. NREL/TP-580-24772
24. Szidat, S., T. M. Jenk, et al. (2004). "Radiocarbon (14C)-deduced Biogenic and Anthropogenic Contributions to Organic Carbon (OC) of Urban Aerosols from Zurich, Switzerland." Atmospheric Environment 35: 4035-4044.
25. Szidat, S., T. M. Jenk, et al. (2004). "Source Apportionment of Aerosols by C-14 Measurements in Different Carbonaceous Particle Fractions." Radiocarbon 46(1): 475-484.
26. Taft, R. W., M. H. Abraham, et al. (1985). "Solubility properties in polymers and biological media 5: an analysis of the physicochemical properties which influence octanol-water partition coefficients of aliphatic and aromatic solutes." Journal of Pharmaceutical Sciences 74(8): 807-14.
27. Tanner, R. L., W. J. Parkhurst, et al. (2004). "Fossil Sources of Ambient Aerosol Carbon Based on 14C Measurements." Aerosol Science and Technology 38(S1): 133-139.
28. Turpin, B. J., P. Saxena, et al. (2000). "Measuring and simulating particulate organics in the atmosphere: problems and prospects." Atmospheric Environment 34(18): 2983-3013.

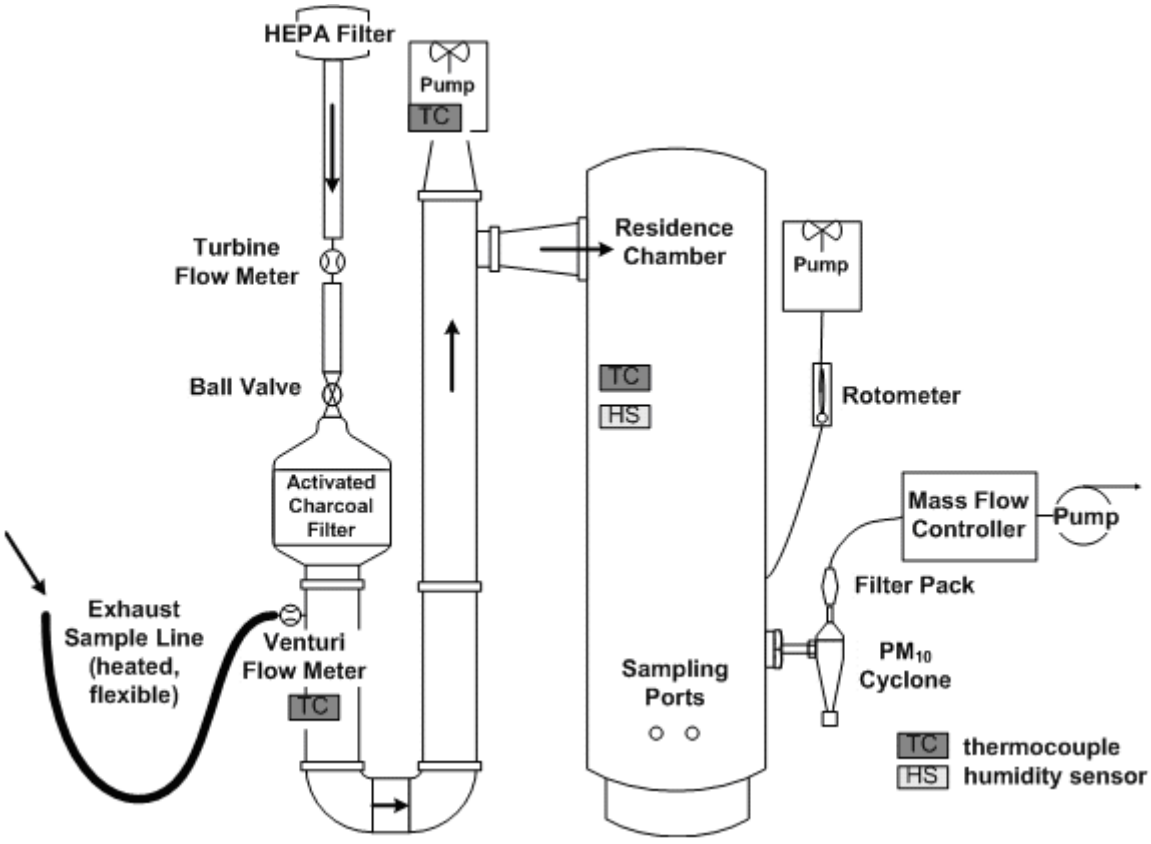

Figure 1. Dilution tunnel schematic.

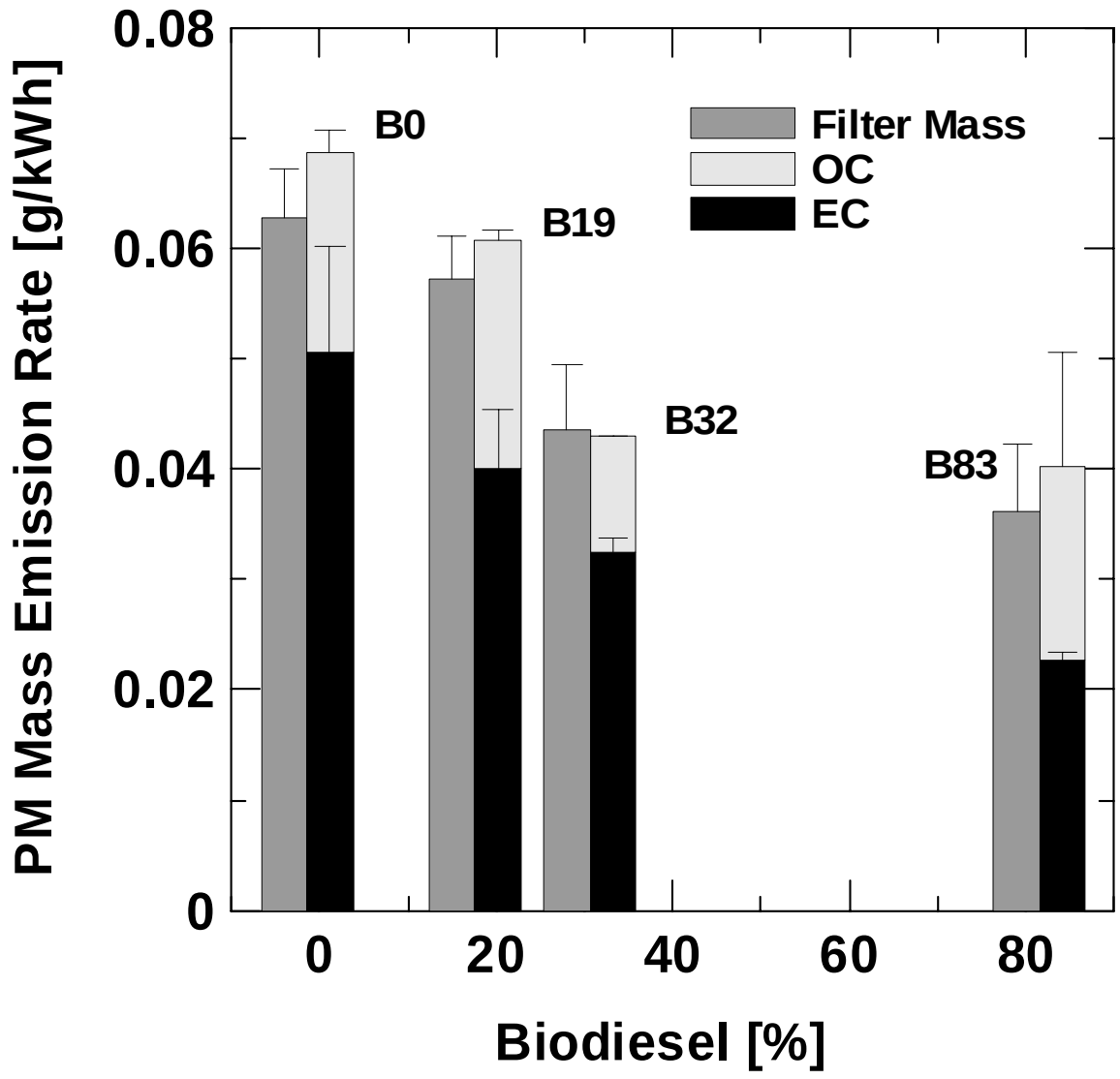

Figure 2. Comparison of gravimetric, OC and EC mass emission rates as a function of fuel biodiesel concentration. Error bars represent one standard deviation.

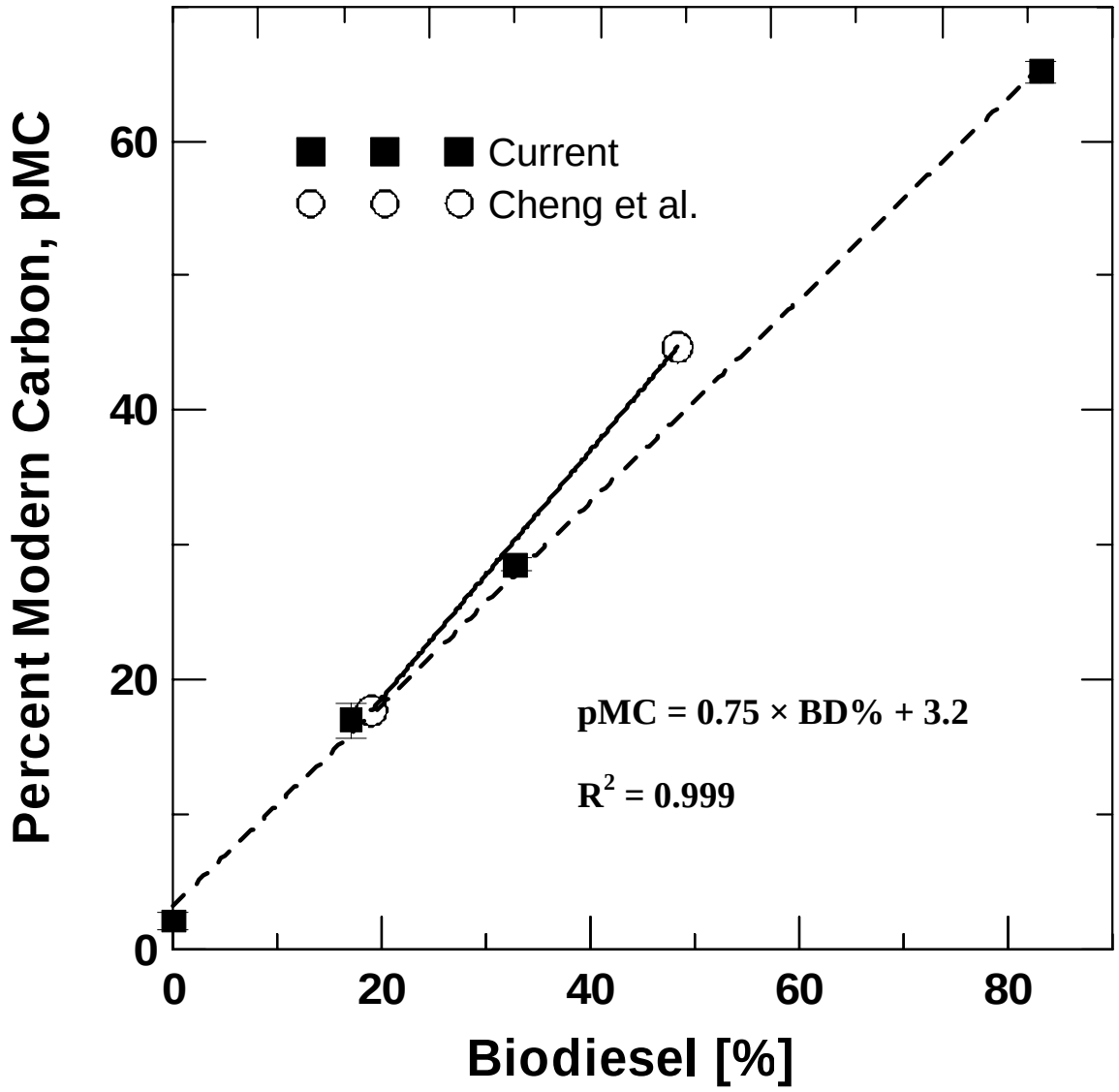

Figure 3. Percent modern carbon (pMC) emitted in the exhaust as a function of pMC in the fuel for this work and Cheng et al. Error bars representing one standard are generally within the size of the data points.

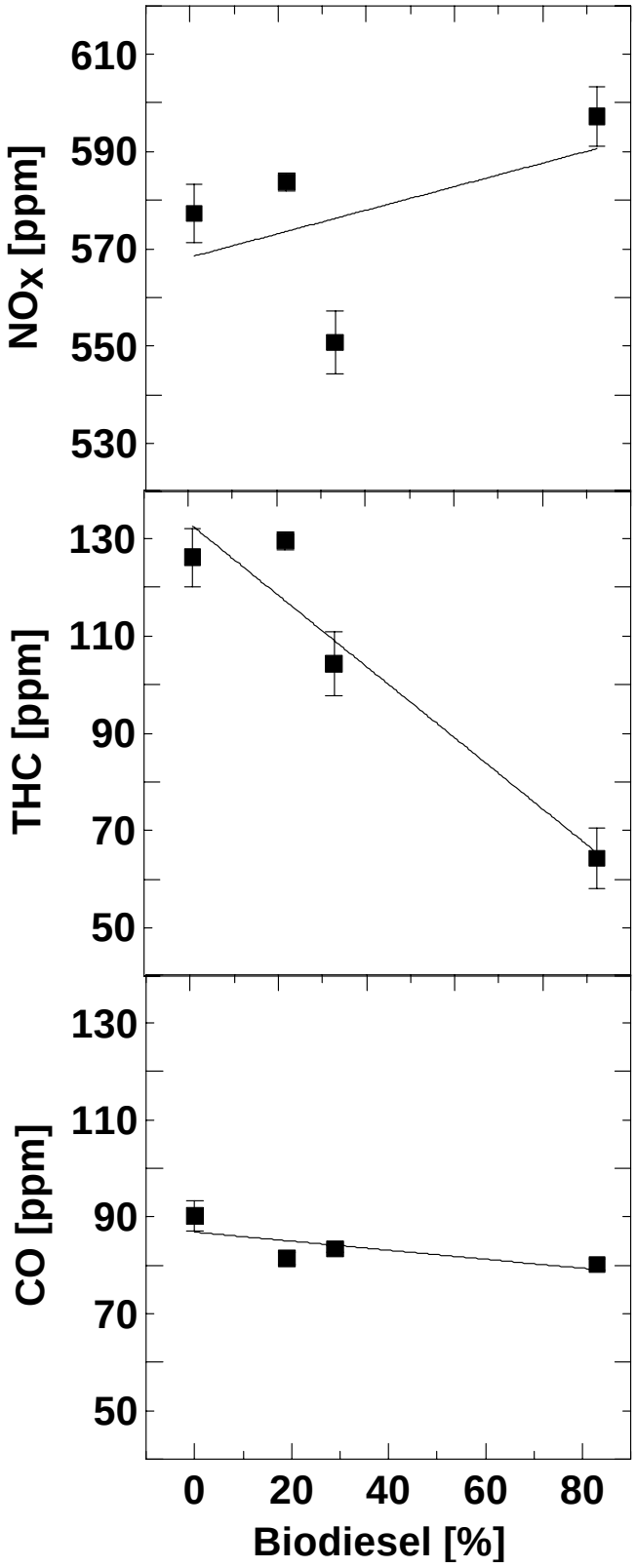

Figure 4. Gaseous NO_x, THC and CO emissions as a function of biodiesel blend percent. Error bars represent one standard deviation.

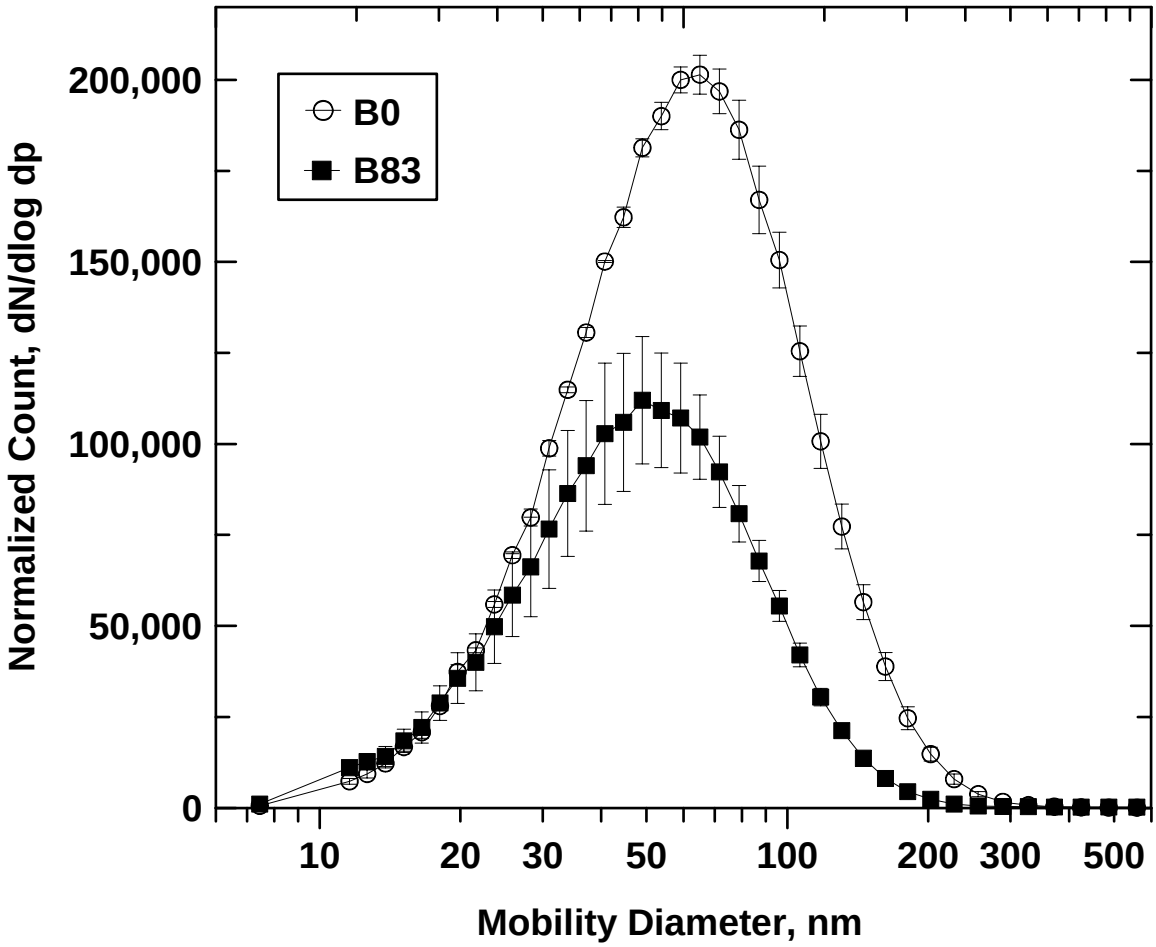

Figure 5. Particle size distribution, by number, determined with an SMPS based on mobility diameter for petrodiesel (B0) and an 83% biodiesel blend (B83). Error bars represent one standard deviation.

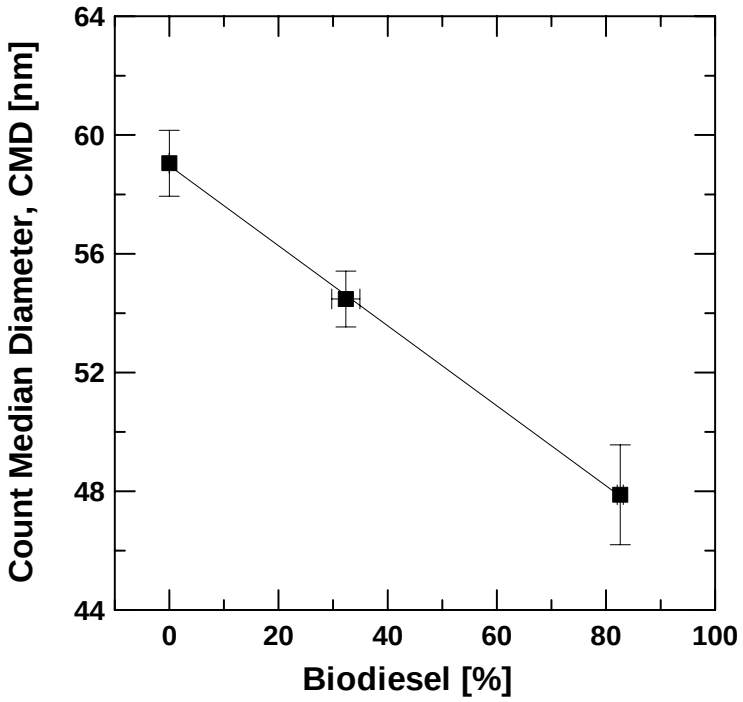

Figure 6. Count median diameter of the particle size distribution as a function of fuel biodiesel content. Error bars represent one standard deviation.

Table 1. Engine testing parameters and measurements.

Variable	**Detail**	*Variation*
Engine	John Deere 4024T, 2.4L	None
Oil	SAE 15W-40	
Fuel	Soy-based Biodiesel	B0, B19, B32, B83
PM Measurement	PM_{10} Mass (Teflon filter) OC/EC, ^{14}C (Quartz + Quartz-behind-Teflon)	2 tests / fuel type
Gas Measurement	THC, CO, CO_2, O_2, NO_x	

Table 2. Comparison of TC, OC and EC [g/kWh] with baseline diesel and Cheng study. Note current TC and OC emission rates from our work have been corrected for the positive adsorption artifact.

	Fuel	TC[a] g/kWh	% Diesel[b]	OC[c] g/kWh	% Diesel	EC[d] g/kWh	% Diesel
Current Study	**B0**	0.0597		0.0092		0.0505	
	B19	0.0493	83%	0.0092	100%	0.0401	79%
	B32	0.0384	64%	0.0059	64%	0.0325	64%
	B83	0.0343	58%	0.0116	126%	0.0227	45%
Cheng et al. (2003)	**B0**	0.0259		0.0125		0.0134	
	B20	0.0189	73%	0.0089	71%	0.0101	75%
	B50	0.0250	96%	0.0128	102%	0.0122	91%
	B100	0.0291	112%	0.0245	196%	0.0046	34%

[a] TC = total carbon
[b] % Diesel provides a relative comparison to baseline emissions of raw petrodiesel
[c] OC = organic carbon
[d] EC = elemental carbon

Table 3. Average percent modern carbon (pMC) filter and fuel measurements ± 1 standard deviation. The corrected pMC_{PC} represents modern, particulate carbon corrected for the vapor adsorption artifact on the quartz filter.

	Fuel pMC	**pMC_{front} [a]**	**pMC_{back} [a]**	**Corrected pMC_{PC}**
B0	0.02% ± 0.04	9.6% ± 0.10	50.7% ± 0.7	2.1%
B19	17.0% ± 0.14	29.3% ± 0.15	70.2% ± 1.0[b]	17.0%
B32	32.8% ± 0.19	32.6% ± 0.20	62.0% ± 1.1	28.6%
B83	83.1% ± 0.26	68.4% ± 0.25	83.6% ± 1.1	65.2%

[a] average of two measurements ± average of both errors

[b] only one filter measurement due to loss of second filter in analysis

Table 4. Gaseous emissions averages and linear trend analysis for various biodiesel blends.

		THC [ppm]	CO [ppm]	NO_x [ppm]	O_2 [%]	CO_2 [%]
Biodiesel %	**0**	126	90.4	577	9.51	8.16
	20	130	81.4	584	9.63	8.25
	29	104	83.3	551	9.85	8.05
	83	64.3	80.2	596	9.72	8.30
Regression Data	**slope**	-0.816	-0.098	0.253	0.002	0.002
	y-int	133	87.1	569	9.61	8.14
	R^2	0.91	0.57	0.22	0.24	0.28
	p-value	**0.04**[a]	0.25	0.51	0.53	0.48

[a] statistically significant at 95% confidence level